Available online at www.sciencedirect.com
ScienceDirect
Applied Geochemistry 22 (2007) 837–850
Applied Geochemistry
www.elsevier.com/locate/apgeochem

Rare earth elements as tracers of sediment contamination by phosphogypsum in the Santos estuary, southern Brazil

Sonia Maria Barros de Oliveira [a,*], Paulo Sergio Cardoso da Silva [b], Barbara Paci Mazzilli [b], Deborah Ines Teixeira Favaro [b], Catia Heloisa Saueia [b]

[a] *Institute of Geosciences, University of São Paulo, rua do Lago 562, 05508-080, São Paulo, Brazil*
[b] *Institute of Nuclear and Energetic Research, IPEN, Caixa Postal 11049, São Paulo, Brazil*

Received 13 June 2006; accepted 8 December 2006
Editorial handling by W. B. Lyons
Available online 7 February 2007

Abstract

In the Cubatão region, southern Brazil, sediments are transported by several rivers from the Serra do Mar Ridge into the Santos estuary. Fertilizer plants have been operating along the margins of one of these rivers (Mogi River) producing a large volume of phosphogypsum, which is stockpiled in nearby areas. Surface sediments of the Mogi River were sampled upstream and downstream in relation to the point where the effluents of the phosphogypsum piles flow into the drainage system. In the vicinity of this point one sediment core was collected. Results show that REE, Ba, Zr and Th concentrations in the non-contaminated sediments are of the same order as those present in the upper continental crust. The contaminated samples present a composition affected by that of the phosphogypsum, marked by a higher concentration of these elements and a stronger degree of REE fractionation. These phosphogypsum characteristics are inherited from the Catalão igneous phosphate ore and were moderately modified by the industrial process of phosphoric acid production. The phosphogypsum signal decreases rapidly downstream, pointing to a limited area of influence of the stacks. The deepest sediments of the core are also free of contamination, representing a time interval prior to the deposition of phosphogypsum wastes on the banks of the estuary.

1. Introduction

Rare earth elements (REE) form a coherent group of trace elements with systematic changes in their chemical properties across the series (Henderson, 1984), allowing only limited mobility and fractionation during weathering and sedimentation (Rolinson, 1993). Consequently, they have been extensively used in studies of provenance of sediments and as tracers of environmental changes, including those of anthropogenic origin (Klaver and van Weering, 1993; Sholkovitz, 1992; Hannigan and Sholkovitz, 2001; Yang et al., 2002; Oliveira et al., 2003; Borrego et al., 2004).

In the Cubatão region, situated less than 100 km from the metropolis of São Paulo, in southern Brazil, sediments are transported by several rivers from the Serra do Mar Ridge into the Santos estuary. The source of the sediments is the Precambrian

* Corresponding author. Fax: +55 11 210 4958.
E-mail address: soniaoli@usp.br (S.M.B. de Oliveira).

0883-2927/$ - see front matter © 2007 Elsevier Ltd. All rights reserved.
doi:10.1016/j.apgeochem.2006.12.017

metamorphic rocks of granitic composition, which belong to the Costeiro Complex (Perrotta et al., 2005). Fertilizer plants have been operating along the margins of some of these rivers producing a large volume of phosphogypsum, a by-product of the production of phosphoric acid, which is disposed of in nearby storage areas, as piles on the margins of the rivers. During the industrial process, phosphogypsum is filtered off and pumped as slurry to nearby ponds, where it remains for a period sufficient to allow complete deposition. The water is not released to the environment because the plants operate in a closed circuit. The phosphogypsum waste is then moved to the so-called gypsum stacks. In the Santos estuary, phosphogypsum is stored at a rate of approximately 4000 ton per day on stacks near the Mogi River. Fig. 1 shows the location of the Mogi River and the Santos estuary.

The phosphate rock originates from the Catalão ultramafic-alkaline carbonatite complex. This complex belongs to a group of Mesozoic alkaline rocks bordering the Paraná basin and consists of a circular stock of approximately 27 km^2, intruded in late Proterozoic Araxá mica schists (Ulbrich and Gomes, 1981). The main rock units recognized in the massif are dunites, peridotites, pyroxenites, phoscorites and carbonatites. New data on one of the rock units enriched in phosphates are presented by Ribeiro et al. (2005). Two phosphate mines and one Nb mine are currently in operation.

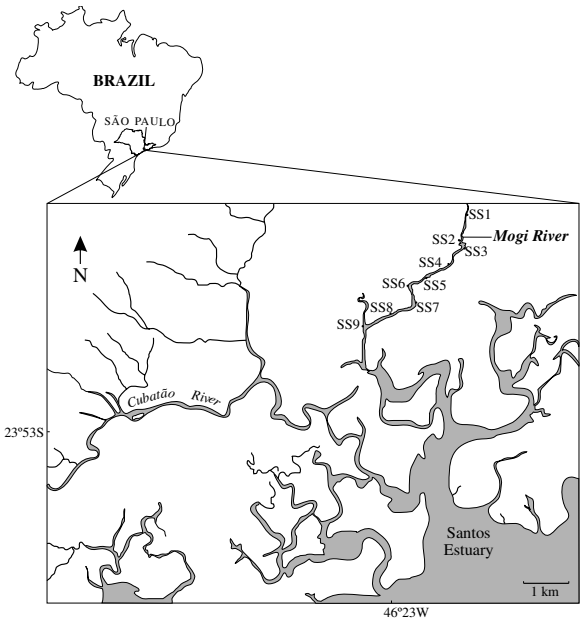

Fig. 1. The Santos estuary setting and sampling locations of surface sediments along the Mogi River.

The mineralogical composition of the phosphate ore is dominated by fluorapatite, goethite and quartz, with minor amounts of Al-phosphates, anatase, magnetite, monazite and barite (Oliveira and Imbernon, 1998). Information on mineralogical and chemical characterization of some of these minerals can be found in Toledo (2000) and Toledo et al. (2004a,b).

In the phosphate mines, the ore is treated by flotation-separation processes in order to concentrate the P content. The phosphate rock concentrate, made up mainly of apatite, is then attacked with H_2SO_4 to produce phosphoric acid, hydrogen fluoride and phosphogypsum. Phosphogypsum consists mainly of gypsum ($CaSO_4{\cdot}2H_2O$) with lesser quantities of impurities which can vary greatly depending on the source of the phosphatic rock used in the process, but generally includes Al, P, F, Si, Fe, Mg and organic matter, especially when the source rock is sedimentary phosphorite (Rutherford et al., 1994). On the other hand, carbonatite ores, enriched in REE, Ba and radionuclides, generate a phosphogypsum with a different geochemical signature. In general, only limited information exists on the composition of phosphogypsum and most of this is for phosphogypsum produced from sedimentary ores, for instance, those from Florida, Togo and Idaho (Rutherford et al., 1995; Arocena et al., 1995), Senegal and Morocco (Martin et al., 1999), and Syria (Al-Masri et al., 2004). In Brazil, radionuclide characterization and other data on the phosphogypsum from Catalão have been given by Mazzilli et al. (2000) and Santos et al. (2006). A similar study on radionuclides and heavy metals was undertaken by Conceição and Bonotto (2006) with the phosphogypsum generated from a phosphate rock of another alkaline massif, Tapira, which belongs to the same province of Catalão. Due to the large quantities produced annually worldwide (5 ton of phosphogypsum per tonne of phosphoric acid) and the appreciable amounts of impurities it can contain, there is a need to more fully understand the chemistry and mineralogy of phosphogypsum in order to define the best waste management strategies and environmental policies.

The objectives of the present study are: (1) to determine the REE, Th and Ba signature of the phosphogypsum produced from the Catalão ore; (2) to investigate the transfer and fractionation processes of REE during phosphogypsum production

through the chemical treatment of the Catalão phosphate rock concentrate, and (3) to demonstrate that REE are adequate tracers for the phosphogypsum contamination of Mogi River sediments.

2. Materials and methods

Six samples of the phosphate rock concentrate (PRC1 to PRC6) and 8 samples of phosphogypsum (PG1 to PG8) were provided by the manufacturers. All samples were dried at a temperature not greater than 45 °C and ground to less than 200 mesh (74 μm).

Nine surface sediment samples were taken from the estuarine area of the Mogi River, from upstream to downstream, along a nearly 3 km stretch (SS1 to SS9) in the region surrounding the fertilizer factory (Fig. 1). In the vicinities of site SS6 (where the effluents of the phosphogypsum stacks enter the drainage system), a 32 cm sediment core was retrieved manually, using a polyethylene tube (internal diameter = 3 cm). The sediment core was conditioned in a plastic bag and maintained frozen until preparation for analysis in the laboratory. The tube was opened with an electric saw and the core was sliced every 2 cm with a plastic device, totaling 16 samples (CS0-2 to CS30-32). Bulk samples, previously dried at 65 °C in a ventilated oven, were ground and sieved through a 150 mesh (105 μm) sieve for chemical analysis.

For the multielemental analyses approximately 150 mg of the samples and approximately 150 mg of reference material and synthetic standards were accurately weighed and sealed in pre-cleaned double polyethylene bags for irradiation and subsequent neutron activation analysis. Single and multielement synthetic standards were prepared by pipetting aliquots of standard solutions (SPEX CERTIPREP) onto small sheets of Whatman no. 41 filter paper. About 1 μg for La and Th, 4 μg for Ce, 2 μg for Nd, 0.5 μg for Sm, Eu, Tb, Yb and Lu, and 500 μg for Ba were used for synthetic standards preparation. Samples, reference materials and synthetic standards were irradiated for 16 h, under a thermal neutron flux of 10^{12} n cm^{-2} s^{-1} in the IEA-R1m nuclear research reactor at IPEN - Instituto de Pesquisas Nucleares, São Paulo, Brazil. Two series of counts were undertaken: the first one, 5–7 days after irradiation (sample-detector distance of 9 cm), and the second one after 15–20 days of decay (sample–detector distance of 3 cm). The counting time for a good statistical counting (less than 5% of error in each peak) was 2 h for each sample and reference materials and 30 min for each synthetic standard. Gamma spectrometry was performed using a Canberra gamma X hyper-pure Ge detector and associated electronics with a resolution of 0.88 keV and 1.90 keV for ^{57}Co and ^{60}Co, respectively.

The analysis of the data was made by using a VISPECT program to identify the gamma-ray peaks and by an ESPECTRO program to calculate the concentrations. Both programs were developed at the Neutron Activation Analysis Laboratory (LAN/CRP), IPEN. The uncertainties of the results were calculated by errors propagation. The precision and accuracy of the analytical technique were evaluated by measuring the reference materials Buffalo River sediment (NIST SRM 2704) and Soil 7 (IAEA) which have certified values for most elements. The detection limits in ppm were: Ba (45), Th (0.18), Zr (73), La (0.4), Ce (1.2), Nd (5), Sm (0.05), Eu (0.08), Tb (0.24), Yb (0.17), Lu (0.03). The relative standard deviation ranges from 1.1% to 8.2% and the relative error, from 3.3% to 10%.

The residues from the aqueous dissolution of two phosphogypsum samples (RPG2 and RPG8, derived from PG2 and PG8, respectively) were analysed by ICP-OES and XRD at the Institute of Geosciences of the University of São Paulo. Chemical determination of Si, Al, Fe^{t}, Mg, Ca, Na, K, P, Mn, Ti, Ba, Sr, La, Ce, Nd, Sm and Zr was performed on an ARL-3410 sequential spectrometer by alkaline fusion of 0.25 g sample powder with 0.75 g flux (lithium tetra and metaborate) with a 1:1000 sample dilution in 2N HNO_3. Three international reference materials – GN-S (granite), JG-1a (granite) and Nist-694 (phosphate rock) – were analysed with the samples. Complete descriptions of these procedures can be found in Janasi et al. (1995). Mineralogical determinations were obtained by XRD, using a Siemens D500 instrument with Cu Kα radiation from 10° to 60° at a rate of 0.05° s^{-1}.

3. Results and discussion

Chemical data on the phosphate rock concentrate (PRC) and phosphogypsum (PG) are presented in Tables 1 and 2. Table 3 shows the mass balance calculations for REE during the industrial process of phosphoric acid production. In Table 4 data on partial chemical composition (S and F were not determined) of the residue of aqueous dissolution of phosphogypsum (RPG) are displayed. Tables 5 and 6 present chemical data for surface (SS) and core sediments (CS). Tables 1 and 5 show concentrations and

Table 1
Rare earth element concentrations (ppm) in the Catalão phosphate rock concentrate (PRC), Catalão phosphogypsum (PG) and other phosphogypsum samples from Florida: A0, A1, A20; Togo: B0, B1 and Idaho: C-95 (Rutherford et al., 1995)

	La	Ce	Nd	Sm	Eu	Tb	Yb	Lu
PRC1	1660	4110	1140	225	62	nd	10.4	0.62
PRC2	1960	5270	1560	254	67	nd	17.7	0.54
PRC3	1720	4070	1530	232	55	8.9	17.4	0.54
PRC4	2510	5410	2250	272	73	19.8	16.6	0.69
PRC5	2470	5870	1170	267	75	10.1	14.6	0.60
PRC6	3000	7150	1310	285	76	13.1	12.1	0.88
mean	2220	5310	1490	256	68	13.0	14.8	0.65
st.dev.	530	1160	410	24	8	4.9	3.0	0.13
PG1	680	1600	710	78	23	5.6	1.0	0.16
PG2	690	1450	690	75	22	5.0	2.9	0.23
PG3	1450	3340	1340	179	45	7.0	2.1	0.26
PG4	1460	3280	1190	175	46	6.5	8.0	0.31
PG5	1140	2820	1280	145	40	6.8	5.3	0.24
PG6	1270	2670	1660	151	35	5.3	7.9	0.20
PG7	1290	2980	790	147	38	7.4	6.3	0.12
PG8	1690	3050	1150	151	37	4.8	6.3	0.23
mean	1210	2650	1100	138	36	6.0	5.0	0.22
st.dev.	360	730	340	40	9	1.0	2.7	0.06
A0	35	54	39	7.3	1.6	1.1	1.8	0.17
A2	37	57	42	7.7	1.7	1.1	1.9	0.21
A20	40	58	43	7.8	1.8	1.2	2.5	0.30
B0	70	129	18	14.1	3.4	2.0	3.7	0.42
B1	41	55	41	7.7	1.8	1.3	2.7	0.32
C9-35	73	20	48	6.9	1.5	1.3	3.3	0.43

Table 2
Trace element, total REE, light REE (La to Eu), heavy REE (Tb to Lu) concentrations (ppm), and LREE/HREE, $(La/Yb)_{CH}$, $(Ce/Ce^{*})_{CH}$, $(Eu/Eu^{*})_{CH}$ ratios in the Catalão phosphate rock concentrate (PRC), Catalão phosphogypsum (PG) and other phosphogypsum samples from Florida: A0, A1, A20; Togo: B0, B1 and Idaho: C-95 (Rutherford et al., 1995)

	Ba	Zr	Th	REE	LREE	HREE	L/H	$(La/Yb)_{CH}$	$(Ce/Ce^{*})_{CH}$	$(Eu/Eu^{*})_{CH}$
PRC1	1630	nd	69	7200	7190	nd	nd	107	1.2	1.1
PRC2	2190	2570	107	9130	9110	nd	nd	74	1.3	1.1
PRC3	2780	2400	123	7630	7610	26.9	283	66	1.1	0.9
PRC4	10240	5090	100	10550	10510	37.1	284	102	1.0	0.9
PRC5	8360	1020	112	9870	9850	25.3	389	113	1.2	1.0
PRC6	13660	1180	110	11840	11820	26.0	454	167	1.2	1.0
mean	6480	2450	103	9370	9350	28.8	353	112	1.2	1.0
st.dev.	5000	1630	19	1760	1760	5.5	84	36	0.1	0.1
PG1	890	1570	37	3100	3090	6.7	460	452	1.1	1.0
PG2	680	1620	34	2920	2920	8.1	360	161	1.0	1.0
PG3	1790	1040	65	6370	6360	9.3	681	461	1.1	0.9
PG4	1630	1170	68	6160	6150	14.8	417	123	1.1	1.0
PG5	1450	2410	70	5430	5420	12.3	440	144	1.1	1.0
PG6	1560	1550	57	5790	5780	13.4	431	107	0.9	0.9
PG7	2690	360	45	5250	5240	13.8	379	136	1.2	0.9
PG8	2350	500	60	6090	6080	11.4	535	180	0.9	0.9
mean	1630	1280	54	5140	5130	11.2	463	220	1.0	1.0
st.dev.	670	660	14	1370	1360	2.9	103	147	0.1	0.1
A0	30	nd	0.7	139	136	3.1	44	13	0.7	0.7
A2	23	nd	1.3	149	145	3.2	45	13	0.7	0.7
A20	43	nd	1.5	154	150	4.0	38	11	0.7	0.7
B0	26	nd	3.6	240	234	6.1	38	13	1.0	0.8
B1	38	nd	1.0	151	147	4.3	34	10	0.6	0.7
C9-35	47	nd	nd	155	150	5.0	30	15	0.1	0.6

Table 3
REE mass balance calculations PRC: mean concentrations (ppm) in the phosphate rock concentrates; PG*1.7: mean concentrations (ppm) in the phosphogypsum, corrected by the dilution factor = 1.7; Gain/Loss (%)

	PRC	PG*1.7	Gain/Loss
La	2220	2057	−7
Ce	5310	4505	−15
Nd	1490	1870	25
Sm	256	235	−8
Eu	68	61	−10
Tb	13	10.2	−22
Yb	14.8	8.5	−43
Lu	0.65	0.37	−43
LREE	9350	8721	−7
HREE	28.8	19.0	−34
REE	9379	8738	−7

mean/standard deviation values for REE, and Tables 2 and 6 show Ba, Zr and Th concentrations, and the sum of total REE (ΣREE), light REE (LREE: La to Eu), heavy REE (HREE: Tb to Lu), (LREE/HREE); also shown are the chondrite normalized ratios $(La/Yb)_{CH}$, $(Ce/Ce^*)_{CH}$, and $(Eu/Eu^*)_{CH}$. For the sake of comparison, in Tables 1 and 2 data are included on phosphogypsum from Florida (A0, A1, A20), Togo (B0, B1) and Idaho (C-95) (Rutherford et al., 1995). Tables 5 and 6 contain data for: North American Shale Composite-NASC (Taylor and McLennan, 1985); Upper Continental Crust-UCC (Taylor and McLennan, 1985); non-contaminated river sediments from China (China 1 and 2: Yang et al., 2002; China 3: Zhu et al., 1997; China 4 and 5: Zhang et al., 1998); river sediments in a non-contaminated area (Spain 1: Borrego et al., 2004) and in a phosphogypsum-contaminated area in the Tinto and Odiel estuary (Spain 2 and 3: Borrego et al., 2004); and WA-world average values for sediments (Bowen, 1979). REE patterns are presented normalized to chondrite and to NASC (Taylor and McLennan, 1985; Gromet et al., 1984; Condie, 1991) in Figs. 2 and 5, respectively.

Table 4
Partial chemical composition (weight %) of the residue of aqueous dissolution of phosphogysum samples (RPG2: residue from PG2 and RPG8: residue from PG8)

	RPG2	RPG8
SiO_2	34.3	22.6
Al_2O_3	1.1	0.3
Fe_2O_3	13.2	8.0
MgO	0.7	0.4
CaO	8.3	7.7
Na_2O	0.01	0.09
K_2O	0.42	0.64
P_2O_5	8.2	4.0
MnO	0.43	0.27
TiO_2	10.7	6.1
Ba	5.4	9.8
Sr	1.4	4.3
La	1.65	2.76
Ce	3.88	6.75
Nd	0.95	1.53
Sm	0.14	0.22
Zr	0.24	1.77

3.1. The phosphate rock concentrate (PRC)

The Catalão phosphate rock concentrate has a geochemical signature characterized by high contents of REE (Table 1), Zr, Ba and Th (Table 2), when compared with the upper continental crust. Mean concentrations of Zr, Ba, Th and ΣREE are 2450 ppm, 6480 ppm, 103 ppm and 9370 ppm, respectively, as compared to 190 ppm, 550 ppm, 10.7 ppm, and 129 ppm, respectively, in the upper continental crust. Moreover, mean values for (LREE/HREE) and $(La/Yb)_{CH}$ ratios are very high (352 and 112, respectively). This strongly fractionated pattern, represented by steep chondrite-normalized REE diagrams (Fig. 2c), is inherited from the parent material, namely, the alkaline-carbonatitic rocks and the phosphate ore of the Catalão massif (Oliveira and Imbernon, 1998).

Average $(Ce/Ce^*)_{CH}$, and $(Eu/Eu^*)_{CH}$ ratios for the PRC are 1.2 and 1.0, respectively (Table 2). Quantitatively, the main REE-carrier in the PRC is apatite (ΣREE up to 1.0 wt%), which is the dominant mineral (Oliveira and Imbernon, 1998; Toledo et al., 2004a); monazite and gorceixite, which are impurities in the Catalão ore, contribute with minor amounts of REE. Thorium occurs as a trace element in monazite (Toledo et al., 2004a), and Ba as a dominant component in gorceixite (Toledo, 2000).

3.2. The phosphogypsum (PG)

The contents of REE, Zr, Ba and Th in the phosphogypsum are not as elevated as those of the phosphate rock concentrate but are significantly higher than those derived from the sedimentary rocks of Florida, Togo and Idaho (Tables 1 and 2). Mean concentrations of Zr, Ba, Th and ΣREE are 1280 ppm, 1630 ppm, 54 ppm and 5140 ppm, respectively. A remarkable feature of the Catalão phosphogypsum is the extremely high degree of REE fractionation, much higher than that of

Table 5
Rare earth element concentrations (ppm) in Mogi River surface sediments (SS), Mogi River core sediments (CS), Upper Continental Crust-UCC, North American Shale Composite-NASC (Taylor and McLennan, 1985), non-contaminated river sediments from China (China 1 and 2: Yang et al., 2002; China 3: Zhu et al., 1997; China 4 and 5: Zhang et al., 1998), WA-world average values for sediments (Bowen, 1979), river sediments in a non-contaminated area (Spain 1: Borrego et al., 2004) and in a phosphogypsum-contaminated area (Spain 2 and 3: Borrego et al., 2004)

	La	Ce	Nd	Sm	Eu	Tb	Yb	Lu
SS1	55	114	44	10	1.3	1.0	3.4	0.56
SS2	60	129	46	11	1.4	1.0	3.2	0.48
SS3	39	95	48	8	1.2	0.6	2.3	0.35
SS4	53	120	64	12	1.3	0.7	2.2	0.37
SS5	46	105	57	13	1.5	0.8	2.8	0.43
SS6	117	275	103	17	2.9	1.0	2.7	0.43
SS7	98	228	87	15	2.5	1.1	2.8	0.42
SS8	69	154	78	13	2.1	0.9	2.8	0.43
SS9	60	140	52	10	1.6	0.9	2.2	0.35
mean	66	151	64	12	1.8	0.9	2.7	0.43
st.dev.	25	61	21	2.8	0.6	0.2	0.4	0.07
CS1-2	165	341	275	24	4.6	1.1	3.6	0.63
CS4-6	357	736	500	45	9.3	1.9	3.5	0.47
CS6-8	454	932	667	56	11.7	3.0	4.0	0.53
CS8-10	201	420	345	26	5.2	1.1	2.8	0.39
CS10-12	103	208	115	14	2.0	0.7	2.4	0.43
CS12-14	106	213	160	15	2.6	1.3	2.9	0.46
CS14-16	153	306	176	21	3.8	0.5	3.5	0.67
CS16-18	201	414	260	26	4.9	1.1	3.6	0.56
CS18-20	375	772	567	47	9.9	4.0	3.9	0.53
CS20-22	374	816	466	50	11.5	2.0	5.4	0.68
CS22-24	206	439	301	30	6.1	1.4	3.5	0.54
CS24-26	142	279	217	21	2.0	1.2	4.4	0.72
CS26-28	47	56	50	9	0.6	0.5	1.9	0.33
CS28-30	36	82	43	7	1.0	0.5	1.9	0.40
CS30-32	42	90	51	8	0.9	0.7	2.7	0.44
CS32-34	39	88	49	7	1.1	0.5	2.5	0.43
mean	188	387	265	25	4.9	1.3	3.3	0.51
st.dev.	135	285	198	16	3.8	1.0	0.9	0.12
UCC	30	64	26	4.5	0.9	0.64	2.20	0.32
NASC	32	73	33	5.7	1.2	0.90	3.10	0.50
China1	40	79	34	6.4	1.3	0.82	2.48	0.35
China2	31	62	27	5.0	1.0	0.65	2.16	0.30
China3	31	64	28	5.1	0.9	0.62	1.01	0.16
China4	47	91	42	6.4	1.1	1.05	2.30	0.39
China5	43	80	35	6.7	1.2	0.97	2.69	0.40
WA	41	83	32	6.4	1.2	1.00	3.60	0.70
Spain1	19	46	21	4.6	1.0	0.59	1.25	0.17
Spain2	91	174	85	15.9	3.6	1.88	4.00	0.63
Spain3	124	232	92	19.3	4.5	2.30	4.90	0.75

samples of phosphogypsum from other reported sources and even higher than those of the Catalão phosphate rock concentrates: mean values for (LREE/HREE) and $(La/Yb)_{CH}$ ratios are 463 and 220, respectively. Chondrite-normalized REE patterns clearly display these corresponding HREE-depleted forms (Fig. 2d). Also shown in this figure are the much less fractionated REE patterns of PG derived from Florida, Togo and Idaho. Average $(Ce/Ce^*)_{CH}$ and $(Eu/Eu^*)_{CH}$ ratios for the PG are 1.0 and 1.0, respectively. Significant positive correlations are observed between ΣREE/Th ($r = 0.88$, $p < 0.05$), ΣREE/Ba ($r = 0.70$, $p < 0.05$) and ΣREE/(LREE/HREE) ($r = 0.50$, $p < 0.10$).

Considering that according to the reaction:

$$Ca_{10}(PO_4) \cdot 6F_2 + 10H_2SO_4 + 20H_2O \rightarrow 10CaSO_4 \cdot 2H_2O + 6H_3PO_4 + 2HF$$

Table 6
Trace element, total REE, light REE (La to Eu), heavy REE (Tb to Lu) concentrations (ppm), and LREE/HREE, $(La/Yb)_{CH}$, $(Ce/Ce^*)_{CH}$, $(Eu/Eu^*)_{CH}$ ratios in Mogi River surface sediments (SS), Mogi River core sediments (CS), Upper Continental Crust-UCC, North American Shale Composite-NASC (Taylor and McLennan, 1985), non-contaminated river sediments from China (China 1 and 2: Yang et al., 2002; China 3: Zhu et al., 1997; China 4 and 5: Zhang et al., 1998), WA-world average for sediments (Bowen, 1979), river sediments in a non-contaminated area (Spain 1: Borrego et al., 2004) and in a PG-contaminated area (Spain 2 and 3: Borrego et al., 2004)

	Ba	Zr	Th	REE	LREE	HREE	L/H	$(LA/Yb)_{CH}$	$(Ce/Ce^*)_{CH}$	$(Eu/Eu^*)_{CH}$
SS1	593	409	20	228	223	4.9	45	11	1.0	0.4
SS2	515	451	24	252	247	4.7	53	13	1.0	0.4
SS3	517	286	23	194	191	3.3	58	11	1.1	0.6
SS4	494	385	25	254	251	3.3	75	16	1.0	0.4
SS5	565	306	24	225	221	4.0	56	11	1.0	0.4
SS6	697	380	22	519	515	4.2	124	29	1.1	0.6
SS7	647	369	23	435	431	4.3	101	24	1.1	0.6
SS8	690	291	23	320	316	4.0	78	17	1.0	0.6
SS9	510	307	23	267	264	3.4	77	19	1.1	0.5
mean	581	354	23	299	295	4.0	74	17	1.0	0.5
st.dev.	80	58	2	109	108	0.6	25	6	0.1	0.1
CS1-2	1050	400	24	815	810	5.3	153	31	0.8	0.7
CS4-6	1490	688	30	1660	1650	5.9	280	68	0.9	0.8
CS6-8	1640	787	32	2130	2120	7.5	282	76	0.9	0.8
CS8-10	1120	443	21	1000	997	4.3	232	48	0.8	0.7
CS10-12	472	434	21	446	443	3.5	126	29	0.9	0.6
CS12-14	639	540	19	501	497	4.7	106	25	0.8	0.6
CS14-16	651	454	23	665	660	4.7	140	29	0.9	0.7
CS16-18	840	523	26	911	906	5.3	171	37	0.9	0.7
CS18-20	1150	819	30	1780	1770	8.4	211	64	0.9	0.7
CS20-22	1390	689	36	1730	1720	8.1	212	46	1.0	0.9
CS22-24	843	483	25	988	982	5.4	182	40	0.9	0.7
CS24-26	689	578	23	667	661	6.3	105	22	0.8	0.3
CS26-28	186	405	10	165	163	2.7	60	17	0.5	0.2
CS28-30	374	301	16	172	169	2.8	60	13	1.0	0.5
CS30-32	368	512	17	196	192	3.8	51	10	0.9	0.3
CS32-34	440	448	17	188	184	3.4	54	11	1.0	0.5
mean	833	532	23	875	870	5.1	170	35	0.9	0.6
st.dev.	434	146	7	637	638	2.0	314	21	0.1	0.2
UCC	550	190	10.7	129	125	3.2	40	9	1.0	0.6
NASC	636	200	12.3	149	145	4.5	32	7	1.0	0.6
China1	nd	nd	nd	164	161	3.7	44	18	0.9	0.6
China2	nd	nd	nd	129	126	3.1	41	10	0.9	0.6
China3	nd	nd	nd	131	129	1.8	72	21	1.0	0.5
China4	nd	nd	nd	191	187	3.7	50	14	0.9	0.5
China5	nd	nd	nd	170	166	4.1	41	11	0.9	0.6
WA	nd	nd	nd	169	164	5.3	31	8	1.0	0.6
Spain1	nd	nd	4.6	94	92	2.0	46	10	1.1	0.7
Spain2	nd	nd	8.7	376	370	6.5	78	15	0.9	0.7
Spain3	nd	nd	10.5	480	472	8.0	59	17	0.9	0.7

approximately 1.7 mass units of phosphogypsum are produced for every mass unit of apatite (phosphate rock concentrate), the mass balance for the REE during the industrial process can be calculated (Table 3). REE gains or losses in phosphogypsum are expressed in percentages in relation to the REE amounts in the phosphate rock concentrate: % gain or loss = (PG*1.7-PCR)*100/PCR. The mean concentrations of REE in phosphogypsum corrected by the dilution factor (PG*1.7) are in general slightly lower than those of the mean phosphate rock concentrate (PCR), with losses limited to approximately 10%, except for HREE with losses of approximately 40% for Yb and Lu. Thus, during the acid processing of the Catalão phosphate rock concentrate, apatite dissolves and LREE are partitioned primarily into the phosphogypsum, while approximately 40% of HREE, go into the

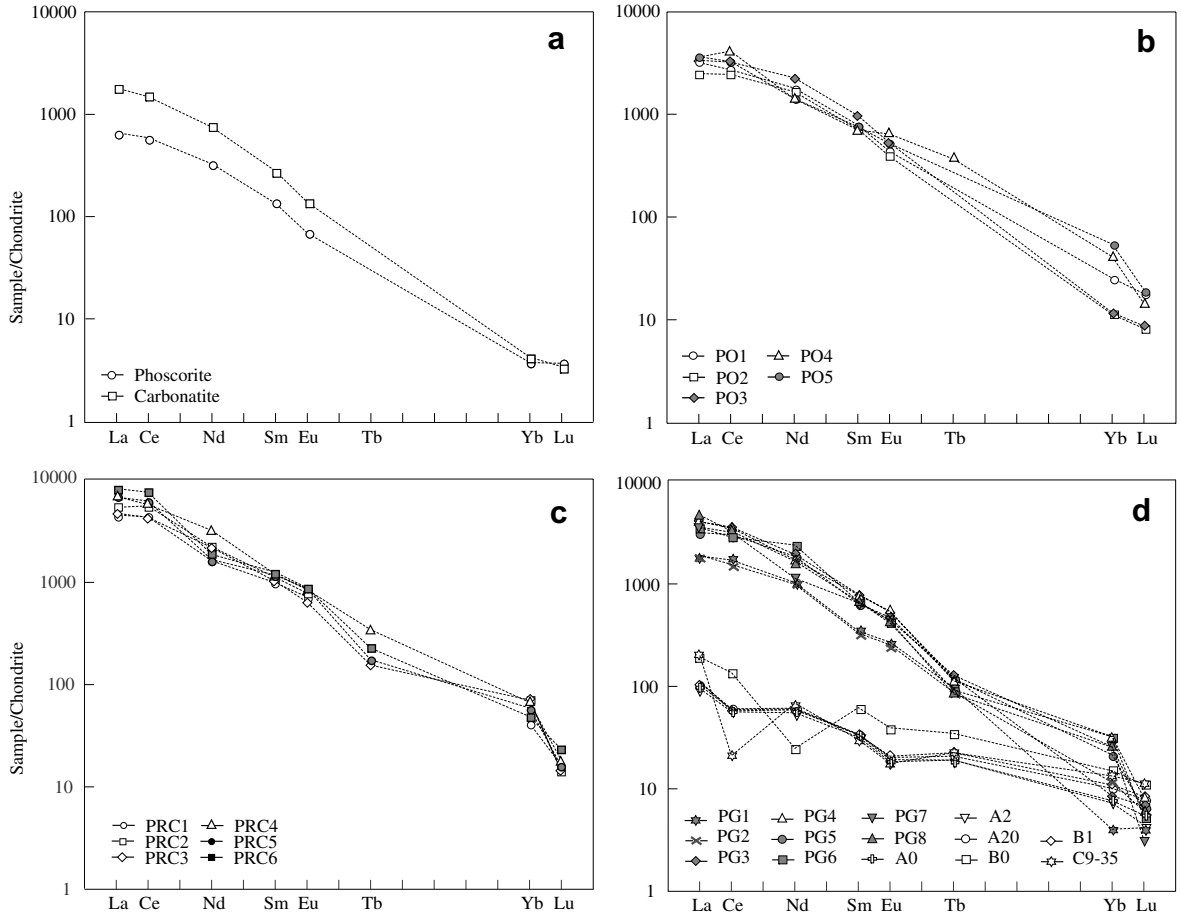

Fig. 2. Chondrite-normalized diagrams: (a) Phoscorite and carbonatite from the Catalão mine, (b) The Catalão ore (PO1–PO5), (c) The phosphate rock concentrate (PRC1–PRC6), (d) Phosphogypsum from Catalão (PG1–PG8), Florida (A0, A2, A20), Togo (B0, B1) and Idaho (C9-35).

phosphoric acid. Similar behavior of REE in other phosphoric acid plants was observed by Andrianov et al. (1976); Berdonosova et al. (1989) and May and Sweeney (1984) (see Rutherford et al., 1994).

In order to investigate the possible REE-carriers in the phosphogypsum, the mineralogical and chemical composition of the residue of aqueous dissolution of two phosphogypsum samples (RPG2 and RPG8) were determined. XRD diffraction showed that these residues contain quartz, minerals of the crandallite group (Al-phosphates of Ca, Sr, Ba and REE), fluorite (CaF_2), strengite ($FePO_4 \cdot 2H_2O$), and minor amounts of gypsum ($CaSO_4 \cdot 2H_2O$) and baryte ($BaSO_4$). The partial chemical composition (S and F were not determined) of RPG2 and RPG8 shows high contents Si, Fe, Ca, P, Ti and LREE (Table 4). These chemical and mineralogical data suggest that at some of the REE in the phosphogypsum is associated with the Al-phosphates of the crandallite-group.

3.3. The surface sediments (SS)

In surface sediments of the Mogi River, the mean Zr concentration is 354 ppm, and ranges from 256 to 451 ppm. Barium and Th mean concentrations are 581 and 23 ppm, ranging from 494 to 697 ppm and 20 to 24 ppm, respectively. These values are of the same order or slightly higher than those reported for UCC and NASC (Table 6). Mean ΣREE concentration (299 ppm) is approximately twice as high as those reported for UCC, NASC and those described in sediments from other non-contaminated fluvial systems (Tables 5 and 6). The same applies for the degree of REE fractionation (mean (LREE/HREE) ratio is 74 and mean $(La/Yb)_{CH}$ ratio is 17).

In general, the distribution of the elements in the surface sediments along the river is fairly homogeneous, except for sites SS6 and SS7, where we can

find the most elevated concentrations and the highest degrees of REE fractionation ((SS6: ΣREE = 519 ppm, (LREE/HREE) = 124; SS7: ΣREE = 435 ppm, (LREE/HREE) = 101)). Average $(Ce/Ce^{*})_{CH}$ and $(Eu/Eu^{*})_{CH}$ ratios for SS are 1.0 and 0.5, respectively, and do not vary significantly along the river.

3.4. The core sediments (CS)

The vertical distributions of Ba, Zr, Th and ΣREE in the core sediments are displayed in Fig. 3. All elements show broadly similar vertical patterns. The highest concentrations are observed in samples located at 4–6, 6–8 cm and 18–20, 20–22 cm, and the lowest values in the deepest samples, corresponding to 26–28, 28–30, 30–32 and 32–43 cm. For Ba, Th, and ΣREE vertical variations are larger than for Zr. The highest Ba concentrations are 1490 ppm (CS4-6), 1640 ppm (CS6-8), 1150 ppm (CS18-20) and 1390 ppm (CS20-22), and the lowest are 186 ppm (CS26-28), 374 ppm (CS28-30), 368 ppm (CS30-32) and 440 ppm (CS32-34). The highest Th concentrations are 30 ppm (CS4-6), 32 ppm (CS6-8), 30 ppm (CS18-20) and 36 ppm (CS20-22), and the lowest are 10 ppm (CS26-28), 16 ppm (CS28-30), 17 ppm (CS30-32) and 17 ppm (CS32-34). The highest ΣREE concentrations are CS4-6 = 1650 ppm, CS6-8 = 2130 ppm, CS18-20 = 1780 ppm, CS20-22 = 1730 ppm, and the lowest concentrations are CS26-28 = 165 ppm, CS28-30 = 172 ppm, CS30-32 = 196 ppm, CS32-42 = 188 ppm. On the other hand, the highest Zr concentrations are 688 ppm (CS4-6), 787 ppm (CS6-8), 819 ppm (CS18-20), 689 ppm (CS20-22), and the lowest concentrations are 405 ppm (CS26-28), 301 ppm (CS28-30), 512 ppm (CS30-32) and 448 ppm (CS40-42). The mean $(Ce/Ce^{*})_{CH}$ ratio is 0.9 and does not vary significantly along the core, contrasting with the $(Eu/Eu^{*})_{CH}$ ratio (mean value of 0.6) which ranges from 0.2 to 0.9.

3.5. The geochemical signature of phosphogypsum in sediments

The relationships between ΣREE and trace elements, (LREE/HREE), $(La/Yb)_{CH}$ and $(Eu/Eu^{*})_{CH}$ ratios in the whole set of sediment samples ($n = 25$) are shown in Fig. 4. These diagrams allow two 2 groups of samples to be distinguished. Group 1 is

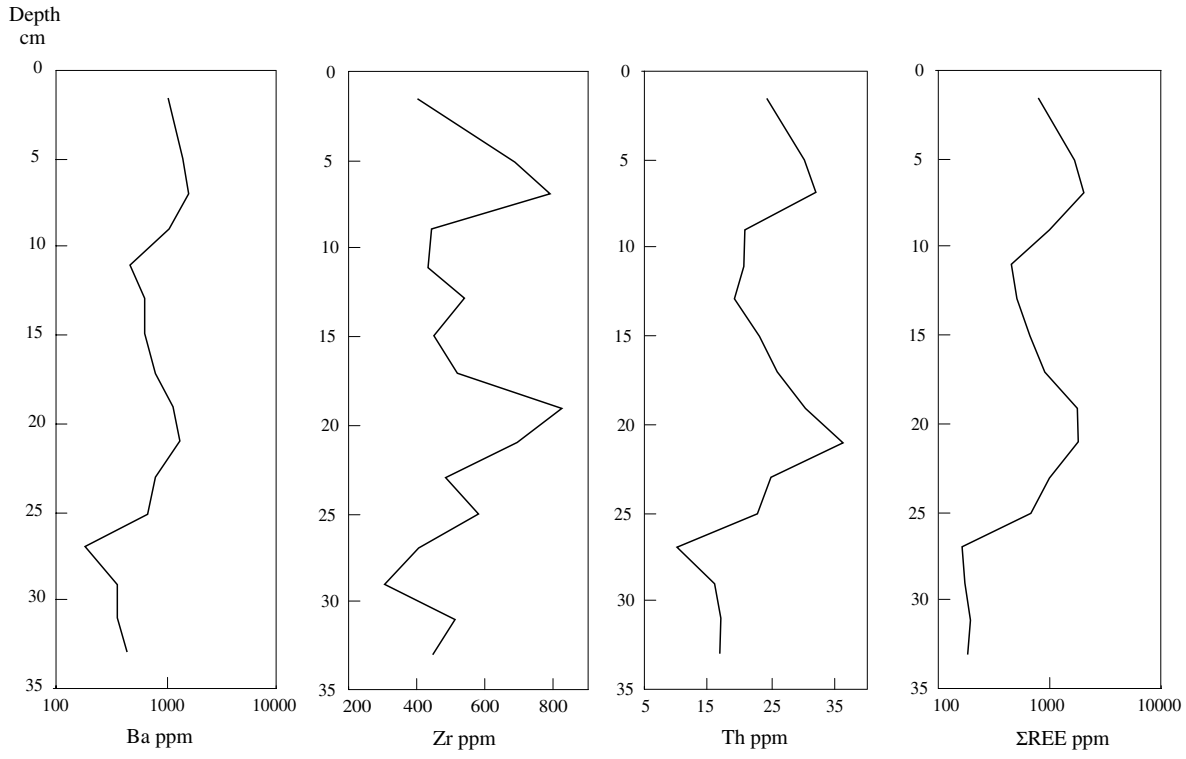

Fig. 3. Vertical distribution of Ba, Zr, Th and ΣREE concentrations in the sediment core.

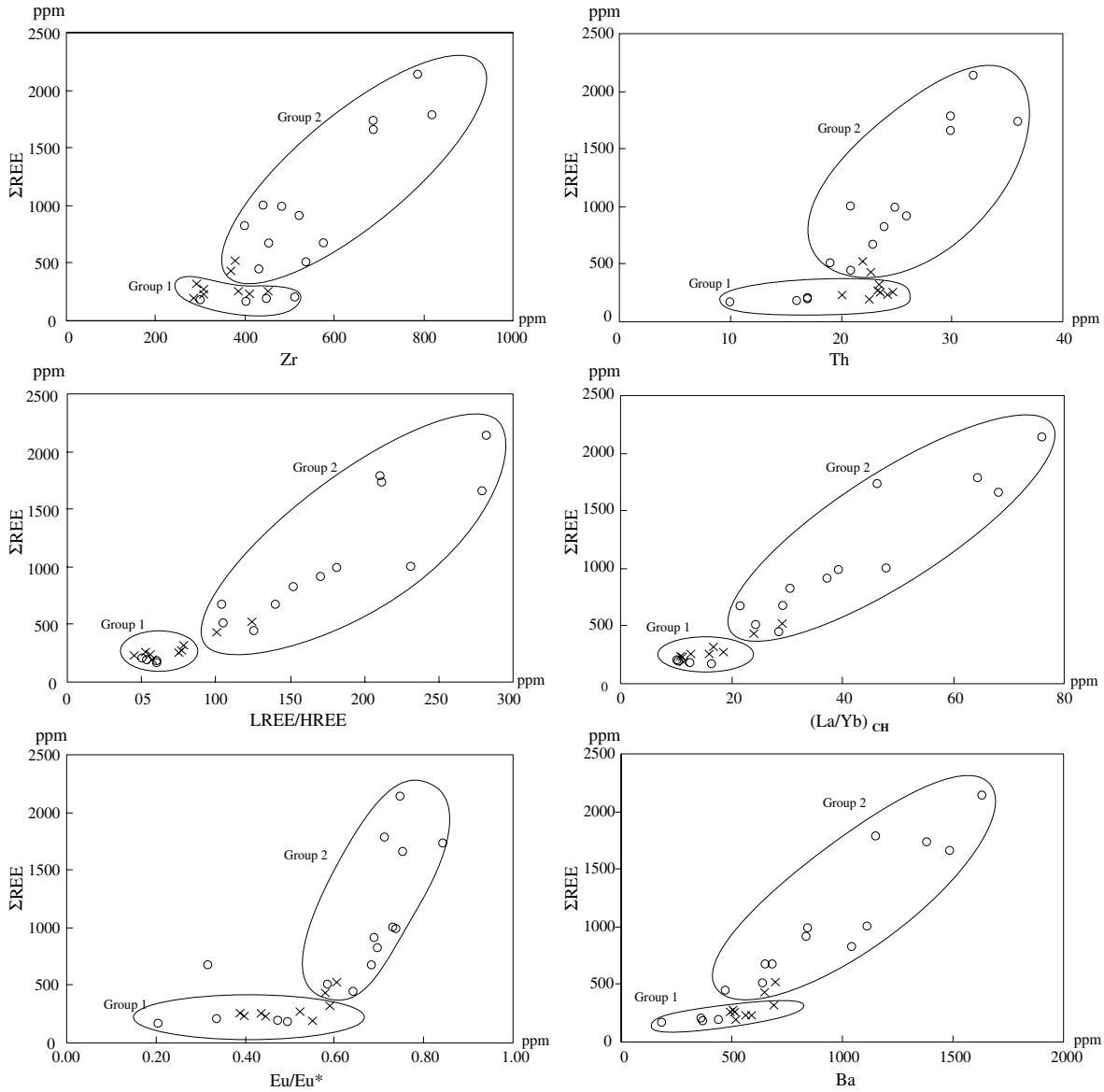

Fig. 4. Relationships between ΣREE and Zr, Th, LREE/HREE, $(La/Yb)_{CH}$, Eu/Eu^* and Ba in surface (×) and core sediments (○).

characterized by samples which REE concentrations are low and vary in a small range (ΣREE between 165 and 320 ppm), in contrast with Group 2 which samples present higher REE contents varying in wider range (ΣREE between 435 and 2130 ppm). Group 1 comprises the samples of the bottom of the core and the surface samples, except for SS6 and SS7. In these samples ΣREE, Zr, Ba and Th concentrations are of the same order of those of NASC, UCC and the non-contaminated sediments from China and Spain (Table 6). No significant correlations are observed between ΣREE and the other variables. $(La/Yb)_{CH}$ ratios are between 10 and 19 and (LREE/HREE) ratios are between 45 and 79. These values are slightly higher than those reported for UCC and NASC. Strong negative Eu anomalies are observed ($(Eu/Eu^*)_{CH}$ ratios are between 0.2 and 0.6). NASC-normalized REE diagrams for samples of this group (Fig. 5a) have a flat but gently inclined pattern marked by a slight enrichment in LREE, and a slight HREE depletion relative to NASC. Fig. 5b displays the NASC-normalized REE patterns for non-contaminated sediments of China and Spain.

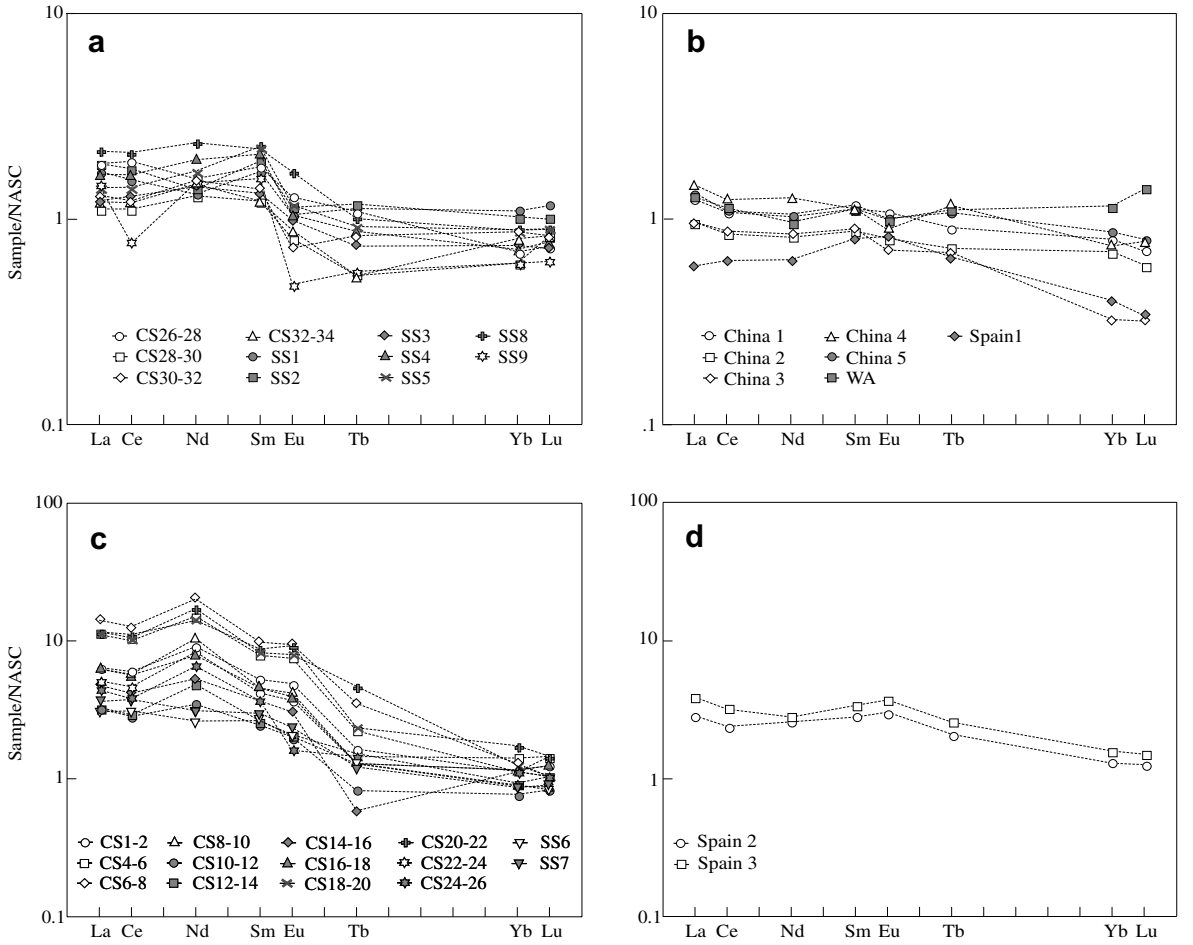

Fig. 5. NASC-normalized diagrams: (a) Group 1 samples, (b) Non-contaminated samples from Spain, China and world average sediments, (c) Group 2 samples, (d) Phosphogypsum-contaminated samples from Spain.

Group 2 is formed by the samples of the core (except for the 4 deepest samples) and SS6 and SS7. ΣREE, Zr, Ba and Th concentrations are much more elevated than those of UCC, NASC and the non-contaminated sediments, and even more elevated than the average values for phosphogypsum-contaminated sediments from the Tinto and Odiel estuary (Table 6). Plots of NASC-normalized REE data (Fig. 5c) show a more pronounced enrichment in LREE, and a slight HREE depletion in Group 2 samples relative to NASC compared not only to Group 1 samples (Fig. 5a), and to other samples of non-contaminated sediments (Fig. 5b), but also to samples of phosphogypsum-contaminated sediments from Spain (Fig. 5d). $(La/Yb)_{CH}$ ratios are between 21 and 69 and (LREE/HREE) ratios are between 93 and 283 meaning that this group of samples shows a higher degree of fractionation compared to the first group. In addition, Eu anomalies are not so pronounced ($(Eu/Eu^*)_{CH}$ ratios are between 0.3 and 0.9). In this group of samples distinct positive correlations are found between ΣREE/Zr ($r = 0.88$, $p < 0.05$), ΣREE/Th ($r = 0.90$, $p < 0.05$), ΣREE/Ba ($r = 0.94$, $p < 0.05$). A clear correlation can also be observed between ΣREE and the variables that express the degree of fractionation: ΣREE/(LREE/HREE) ($r = 0.89$, $p < 0.05$), $\Sigma REE/(La/Yb)_{CH}$ ($r = 0.93$, $p < 0.05$). These relationships indicate that samples with greater REE concentrations also typically exhibit greater fractionation of the REE. Significant correlation occurs between $\Sigma REE/(Eu/Eu^*)_{CH}$ ($r = 0.60$, $p < 0.05$), indicating that the Eu anomaly size decreases with increasing REE abundance.

Group 1 comprises the samples situated upstream in relation to the point where the effluents of the

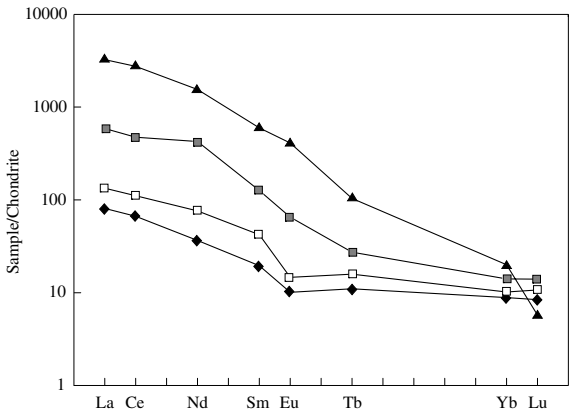

Fig. 6. Chondrite-normalized patterns: average Catalão phosphogypsum (▲), upper continental crust (♦), average contaminated sediments (■), average non-contaminated sediments (□).

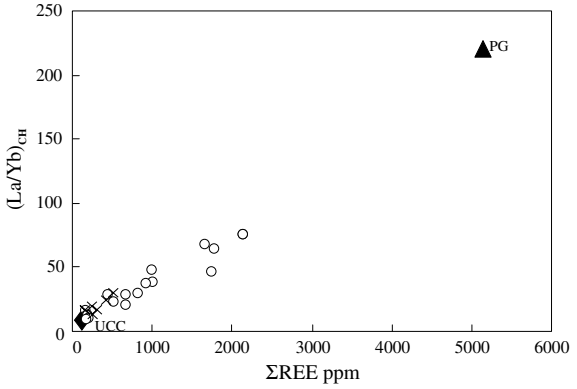

Fig. 7. ΣREE versus $(La/Yb)_{CH}$: surface sediments (×), core sediments (○), average Catalão phosphogypsum (▲PG), upper continental crust (♦ UCC).

phosphogypsum stacks enter the Mogi River (SS1 to SS5), the samples situated downstream in relation to this point, but far from it (SS8 and SS9), and the deepest samples of the core (CS26-28 to CS 32-34), and represents the background for the region.

Group 2, on the other hand, reflects the local influence of PG wastes. It comprises the SS samples situated just where the effluents of the phosphogypsum stacks enter into the Mogi River (SS6) and in the next sampling point downstream (SS7), and the samples from the core (CS1-2 to CS24-26), except for the deepest ones. This group can be seen as a product of mixing between two end-members. One, the dominant, is the source rock of the sediments, whose REE and trace element composition is similar to that of UCC, and the other is PG, present in variable amounts in these samples.

Accordingly, the resultant REE pattern is intermediate between the UCC pattern with low concentrations of REE (ΣREE = 129 ppm), moderate degree of fractionation ($(La/Yb)_{CH} = 9$), and Eu negative anomalies ($(Eu/Eu^*) = 0.6$), and the PG pattern with higher concentrations of REE (ΣREE = 5140 ppm), higher degree of fractionation ($(La/Yb)_{CH} = 220$), and no Eu negative anomalies ($(Eu/Eu^*) = 1.0$). The relationships between the REE patterns for UCC, PG and the averages for contaminated and non-contaminated samples are illustrated by Fig. 6. The intermediate position of the contaminated sediment samples between PG and UCC is also shown in the ΣREE versus $(La/Yb)_{CH}$ diagram (Fig. 7).

4. Conclusions

REE, Ba, Zr and Th concentrations in the non-contaminated sediments of the Mogi River are of the same order as those present in UCC and NASC. In the vicinity of the point where the effluents of the phosphogypsum stacks enter into the Mogi River, the sediment composition is affected by that of PG which presents a typical signature, marked by a much higher concentration of these elements and a stronger degree of REE fractionation. These PG characteristics are inherited from the Catalão igneous phosphate ore and moderately modified by the industrial process of phosphoric acid production. In Brazil, most phosphate ore is derived from alkaline rocks, in contrast with most countries where the more abundant phosphate ore is phosphorite of sedimentary origin, with a quite distinct geochemical signature.

The contaminated sediments of the Mogi River have REE and Th concentrations slightly higher than those from the PG-contaminated sediments of the Tinto and Odiel estuary. Their REE compositions are thought to result from mixing of two end members: the granitic rocks from the Costeiro Complex which are the main source of the sediments and the PG stockpiled on the Mogi River margins. The main REE carrier in the granitic rocks is the mineral zircon. In the PG there is a strong association between REE, Ba and Th with phosphates, which is transferred to the sediments. The phosphogypsum fingerprint is also indicated by a less pronounced Eu anomaly in sediments compared to NASC and UCC. The Eu negative anomaly, a typical crustal signal, present in non-contaminated samples, is diluted by the presence of PG in the contaminated sediments.

The PG signal dies out rapidly downstream (SS8, just 400 m from SS7 shows no sign of contamination), meaning that the area of influence of the PG stacks is limited. The deepest sediments of the core are also free of contamination, representing a time interval prior to the deposition of PG wastes on the banks of the estuary. The vertical variation of REE concentrations across the core seems to be related to the variable intensity of PG transfer into the Mogi River with time.

Acknowledgements

We thank Dr. Johannensson and Dr. Wood for critical reviews of the manuscript and the Brazilian agencies FAPESP and CNPq for financial support.

References

Al-Masri, M.S., Amin, Y., Ibrahim, S., Al-Bich, F., 2004. Distribution of some trace metals in Syrian phosphogypsum. Appl. Geochem. 19, 747–753.

Andrianov, A.M., Rusin, N.F., Burtnenko, L.M., Fedorenko, V.D., 1976. Influence of the main processe parameters on the effectiveness of leaching of rare earth elements from phosphogypsum by sulfuric acid. J. Appl. Chem. USSR 49, 656–658.

Arocena, J.M., Rutherford, P.M., Dudas, M.J., 1995. Heterogeneous distribution of trace elements and fluorine in phosphogypsum by-product. Sci. Total Environ. 162, 149–160.

Berdonosova, D.G., Burlakova, D.G., Yasenkova, M.A., Ivanov, L.N., Melikhov, I.V., 1989. Characteristics of transfer of europium ions from phosphoric acid solution into the $CaSO_4.0.5H_2O$ solid phase. J. Appl. Chem. USSR 62, 211–216.

Borrego, J., López-González, N., Carro, B., Lozano-Soria, O., 2004. Origin of the anomalies in Light and middle REE in sediments of an estuary affected by phosphogypsum wastes (south-westen Spain). Mar. Pollut. Bull. 49, 1045–1053.

Bowen, H.J.M., 1979. Environmental Chemistry of the Elements. Academic Press, London.

da Conceição, F.T., Bonotto, D.M., 2006. Radionuclides, heavy metals and fluorine incidence at Tapira phosphate rocks, Brazil, and their industrial (by) products. Environ. Pollut. 139, 232–243.

Condie, K.C., 1991. Another look at rare earth elements in shales. Geochim. Cosmochim. Acta 55, 2527–2531.

Gromet, L.P., Dymek, R.F., Haskin, L.A., Korotev, R.L., 1984. The "North American shale composite": Its compilation, major and trace element characteristics. Geochim. Cosmochim. Acta 48, 2469–2482.

Hannigan, R.E., Sholkovitz, E.R., 2001. The development of middle rare earth element enrichments in freshwaters: weathering of phosphate minerals. Chem. Geol. 175, 495–508.

Henderson, P., 1984. General geochemical properties and abundances of the rare earth elements. In: Henderson, P. (Ed.), Rare Earth Element Geochemistry. Elsevier, Amsterdam.

Janasi, V.A., Andrade, S., Ulbrich, H.H.G.J., 1995. A correção do drift instrumental em ICP-AES com espectrômetro seqüencial e a análise de elementos maiores, menores e traços em rochas. Bol. IG-USP Ser. Cient. 26, 45–58.

Klaver, G.T., van Weering, T.C.E., 1993. Rare earth element fractionation by selective sediment dispersal in surface sediments: the Skagerrak. Mar. Geol. 111, 345–359.

Martin, J.E., Garcia-Tenorio, R., Respaldiza, M.A., Ontalba, M.A., Bolívar, J.P., da Silva, M.F., 1999. TTPIXE analysis of phosphate rocks and phosphogypsum. Appl. Radiat. Isot. 50, 445–449.

May, A., Sweeney, J.W., 1984. Evaluation of radium and toxic element leaching characteristics of Florida phosphogypsum stockpiles. ASTM Special Tech. Publ., 140–159.

Mazzilli, B.P., Palmiro, V., Saueia, C., Nisti, M.B., 2000. Radiochemical characterization of Brazilian phosphogypsum. J. Environ. Radioact. 49, 113–122.

Oliveira, S.M.B., Imbernon, R.A., 1998. Weathering alteration and related REE concentration in the Catalão I carbonatite complex, central Brazil. J. S. Am. Earth Sci. 11, 379–388.

Oliveira, S.M.B., Larizzatti, F., Favaro, D.I.T., Moreira, S.R.D., Mazzilli, B.P., Piovano, E.L., 2003. Rare earth element patterns in lake sediments as studied by neutron activation analysis. J. Radioanal. Nucl. Chem. 258, 531–535.

Perrotta, M.M., Salvador, E.D., Lopes, R.C., D'Agostino, L.Z., Peruffo, N., Gomes, S.D., Sachs, L.L.D., Meira, V.T., Lacerda, J.V., 2005. Mapa geológico do estado de São Paulo (Geologic map of the state of São Paulo), scale 1: 750 000, CPRM, São Paulo.

Ribeiro, C.C., Brod, J.A., Junqueira-Brod, T.C., Gaspar, J.C., Petrinovic, I.A., 2005. Mineralogical and field aspects of magma fragmentation deposits in a carbonate-phosphate magma chamber: evidence from the Catalão I complex, Brazil. J. S. Am. Earth Sci. 18, 355–369.

Rolinson, H.R., 1993. Using Geochemical Data: Evaluation, Presentation, Interpretation. Longman Scientific Publications.

Rutherford, P.M., Dudas, M.J., Samek, R.A., 1994. Environmental impacts of phosphogypsum. Sci. Total Environ. 149, 1–38.

Rutherford, P.M., Dudas, M.J., Arocena, J.M., 1995. Radioactivity and elemental composition of phosphogypsum produced from three phosphate rock sources. Waste Manag. Resour. 13, 407–423.

Santos, A.J.G., Mazzilli, B.P., Favaro, D.I.T., Silva, P.S.C., 2006. Partitioning of radionuclides and trace elements in phosphogypsum and its source materials based on sequencial extraction methods. J. Environ. Radioact. 87, 52–61.

Sholkovitz, E.R., 1992. Chemical evolution of rare earth elements: fractionation between colloidal and solution phases of filtered river water. Earth Planet. Sci. Lett. 114, 77–84.

Taylor, S.R., McLennan, S.M., 1985. The continental crust: Its composition and evolution. Blackwell Scientific Publications.

Toledo, M.C.M., 2000. O grupo da crandallita no manto laterítico sobre o maciço carbonatítico de Catalão I, GO-Brasil. Geochem. Brasil 14, 71–95.

Toledo, M.C.M., Lenharo, S.L.R., Ferrari, V.C., Fontan, F., Parsefal, P., 2004a. The compositional evolution of apatite in the weathering profile of the Catalão I alkaline-carbonatitic complex, Goias, Brazil. Can. Miner. 42, 1239–1258.

Toledo, M.C.M., Oliveira, S.M.B., Fontan, F., Ferrari, V.C., Parsefal, P., 2004b. Mineralogia, morfologia e cristaloquímica

da monazita de Catalão I (GO, Brasil). Rev. Bras. Geoci. 34, 135–146.

Ulbrich, H.H.G.J., Gomes, C.B., 1981. Alkaline rocks from continental Brazil. Earth Sci. Rev. 17, 135–154.

Yang, S.Y., Jung, H.S., Choi, M.S., Li, C.X., 2002. The rare earth element composition of the Changjiang (Yangtze) and Huanghe (Yellow) river sediments. Earth Planet. Sci. Lett. 201, 407–419.

Zhang, C., Wang, L., Zhang, S., 1998. Geochemistry of rare earth elements in the mainstream of the Yangtze River, China. Appl. Geochem. 13, 451–462.

Zhu, W., Kennedy, M., de Leer, E.W.B., Zhou, H., Alaerts, G.J.F.R., 1997. Distribution and modeling of rare earth elements in Chinese river sediments. Sci. Total Environ. 204, 233–243.